Performance of Nb₃Sn RRP Strands and Cables Based on a 108/127 Stack Design

E. Barzi, G. Ambrosio, N. Andreev, R. Bossert, R. Carcagno, S. Feher, V.S. Kashikhin,
V.V.Kashikhin, M.J. Lamm, F. Nobrega, I. Novitski, Y. Pishalnikov, C. Sylvester, M. Tartaglia,
D.Turrioni, R. Yamada, A.V. Zlobin, M. Field, S. Hong, J. Parrell, Y. Zhang

Abstract—**The high performance Nb₃Sn strand produced by Oxford Superconducting Technology (OST) with the Restack Rod Process (RRP) is presently considered as a baseline conductor for the Fermilab's accelerator magnet R&D program. To improve the strand stability in the current and field range expected in magnet models, the number of subelements in the strand was increased by a factor of two (from 54 to 108), which resulted in a smaller effective filament size. The performance of the 1.0 and 0.7 mm strands of this design was studied using virgin and deformed strand samples. 27-strand Rutherford cables made of 1 mm strand were also tested using a superconducting transformer, small racetrack and 1-m shell-type dipole coils. This paper presents the RRP strand and cable parameters, and reports the results of strand, cable and coil testing.**

Index Terms— **Nb₃Sn, Restack Rod Process, Rutherford cable, Small racetrack coil.**

I. INTRODUCTION

FERMILAB is developing a new generation of accelerator magnets based on Nb₃Sn superconductors and the wind-and-react technology [1]. After attaining success in a 10 T dipole mirror made of 1 mm Powder-in-Tube (PIT) Nb₃Sn strands with modest critical current density and a quite small filament size of ~50 μm, the same results were reproduced in three subsequent 10 T PIT dipoles [2]-[4]. The next step in the high field magnet R&D was to increase the dipole field to the design value of 11 T by using higher performance Restack Rod Process (RRP) strands developed and produced by Oxford Superconducting Technology (OST) for High Energy Physics applications [5]. The baseline OST RRP strand has a 54/61 (i.e. 54 subelements in a 61 stack array) stack design with 70-100 μm of subelement size in 0.7-1.0 mm strand. This strand design and technology, which is commercially produced, demonstrated a record critical current density above 3 kA/mm² at 12 T and 4.2 K. However, due to the high J_c and

quite large subelement size, this strand suffered also from a serious instability problem at low fields [6]-[7]. It was also shown that in cables this problem was enhanced by subelement deformation [6] and sometimes subelement merging [8].

To improve the Nb₃Sn strand stability in the current and field range expected in Fermilab's 11 T magnet models, OST developed a new 1 mm RRP strand of 108/127 stack design with a reduced subelement size. Samples of this strand were also drawn down to 0.7 mm diameter, and both round and rolled samples of 1.0 and 0.7 mm strands were characterized. In addition, Rutherford cables were made using 1 mm strand and tested at self-field. Based on the positive results of strand and cable tests, a small racetrack and a shell-type dipole coil were fabricated and tested. This paper describes the parameters of the new RRP strands and cables, and reports the results of strand, cable and racetrack testing. The results of the shell-type coil test in a mirror configuration will be reported separately.

II. STRAND AND CABLE DESCRIPTION

The strand cross section of the RRP with 108/127 stacks is shown in Fig. 1 (right), where it is compared to the baseline 54/61 stack design (left). The parameters of 1.0 and 0.7 mm strands of the new design are reported in Table I.
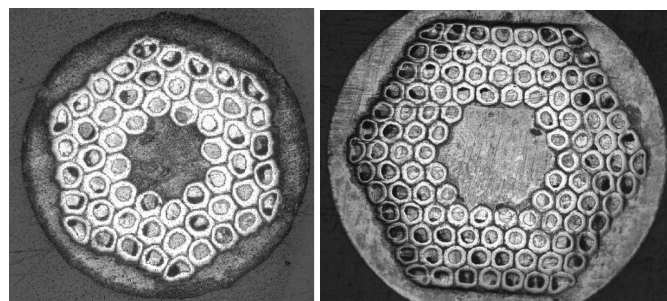

Fig. 1. 54/61 (left), and 108/127 restack (right) RRP designs.

The 108/127 stack RRP strand uses subelements made of pure Nb and discreet Nb-47%Ti filaments, which allows forming (Nb,Ti)₃Sn with high critical current density at high upper critical field. With these subelements and an appropriate heat treatment, this RRP strand provided a nominal J_c of ~2400 A/mm² at 12 T and Cu-matrix RRR above 200 [9].

TABLE I
STRAND PARAMETERS

Strand diameter, mm	0.7	1.0
$J_c(4.2K, 12\ T)$, A/mm^2	~2400	~2400
Geometric subelement size, μm	45-53	64-75
RRR	~200	~300
Twist pitch, mm	12	12
Cu fraction, %	49	49

The 1 mm RRP strand of 108/127 stack design was used to fabricate 27-strand cables with rectangular (RC) and keystoned (KS) cross sections. The KS cable was made by further compacting the RC cable after a short annealing at 190°C in air. The parameters of both cables are described in Table II, and the cable cross sections are shown in Fig. 2.

TABLE II
CABLE PARAMETERS

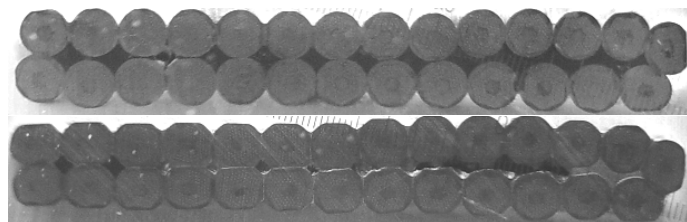| Cable ID	RC	KS
No. of strands	27	27
Strand diameter, mm	0.999±0.003	0.999 ± 0.003
Average width, mm	13.95	14.24
Average thickness, mm	1.95	1.801
Keystone angle, degree	0	0.91
Average lay angle, degree	14.5	14.5
Packing factor, %	81	86

Fig. 2. Rectangular (top) and keystone (bottom) cable cross sections.

III. STRAND STUDIES

Strand samples were tested at 4.2 K round and rolled with 30% deformation. The 1 mm strand was rolled down to 0.7 mm, and the 0.7 mm strand to 0.5 mm. The critical current, I_c, was determined from the voltage-current (V-I) curve using the 10^{-14} Ω·m resistivity criterion. The stability current, I_S, was obtained through sweeping field (V-H) tests [10] as the minimum quench current in the presence of a magnetic field variation. All samples were reacted and tested using standard cylindrical barrels made of Ti-alloy. The details of the V-I and V-H test procedures used are described in [6]. To test I_c and I_S in the rolled strand, two sample orientations with respect to the external magnetic field were used. These are the short edge configuration, where the longest size of the rolled strand is perpendicular to the field, and the long edge configuration, where the strand shortest size is perpendicular to the field.

Table III shows the results for $I_c(12\ T)$, I_S, and RRR for samples that received a final heat treatment (HT) step of 635°C for 60 h. Samples of 1.0 and 0.7 mm round strands showed high RRR, slightly lower than nominal $J_c(12T)$ and high J_S. The J_S of the 0.7 mm strand was much larger than that of the 1 mm strand due to the smaller subelement size. Rolled strands of both sizes showed a low I_c degradation and substantial RRR reduction. Some concern on the smaller size

strand possibly exhibiting more subelement merging was raised by the similar I_S results obtained in the long and short edge configurations. In the absence of merging, a strand tested on the long edge is not expected to be less stable than when tested on the short edge. In addition, for the 0.7 mm strand a RRR reduction by a factor of 6 was observed as opposed to a reduction by a factor of 3 for the 1 mm wire.

TABLE III
MEASURED PROPERTIES OF ROUND AND ROLLED 108/127 RRP STRANDS

Sample geometry	Round	Rolled	Rolled	Round	Rolled	Rolled
Size	1 mm	0.7 mm	0.7 mm	0.7 mm	0.5 mm	0.5 mm
Test configuration	-	Long E.	Short E.	-	Long E.	Short E.
$I_c(12\ T)$, A	880	878	778	437	428	415
$J_c(12\ T)$, A/mm^2	2197	2192	1942	2227	2181	2114
I_S, A	1650	1750	1400	1300	850	900
J_S, A/mm^2	4119	4369	3495	6623	4331	4586
RRR	318	125	94	190	29	31

Magnetization of the 1 mm strand was measured using a balanced coil magnetometer as described in [11]. The effective subelement diameter, d_{eff}, was obtained from 13-10-13 T loops using the magnetization value $\mu_0M(12T)$ per total strand volume and the strand critical current $I_c(12T)$, and considering the subelements round. The d_{eff} was 84±5 μm for the 1 mm RRP strand with 108/127 stack design, comparable as expected with the 85±5 μm of the baseline 0.7 mm RRP strand with half the number of sub-elements (54/61 stack).

Fig. 3 shows the magnetization curves per SC volume for the new 1 mm and baseline 0.7 mm strands between 0 and 3 T. One can see that flux jumps are smaller in amplitude and extend up to a lower magnetic field for the new RRP strand. Since the values of critical current density and effective filament size for the two tested strands were very close, this effect is to be attributed to the higher RRR obtained for the new strand despite using a very similar HT cycle.
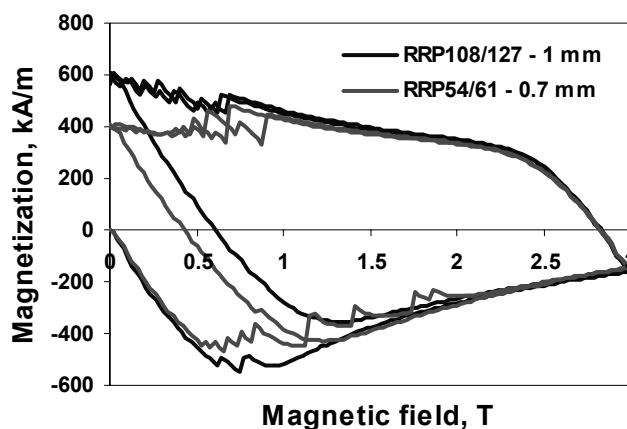

Fig. 3. Magnetization curves per SC volume of a 1 mm RRP strand with 108/127 design compared with a 0.7 mm RRP strand with 54/61 design.

IV. CABLE QUALIFICATION

Rutherford cables were fabricated from 1 mm strands using Fermilab's cabling machine [12]. A set of round and extracted strands were used to characterize both the rectangular and keystoned cables. Sample reaction (final HT step of 645°C for

60 h) and tests at 4.2 K were performed using cylindrical barrels made of either Ti-alloy or stainless steel (SS).

The results of critical current measurements at high fields as a function of magnetic field are shown in Fig. 4. It is intriguing that the I_c degradation of extracted strands was negligible for both cables when tested on SS barrels, but of ~15% when tested on Ti-alloy barrels. This effect was also observed when testing witness samples for the coils (see Table V). The RRR reduction in extracted strands (as averaged along the strand sample) was between 10% and 30%.
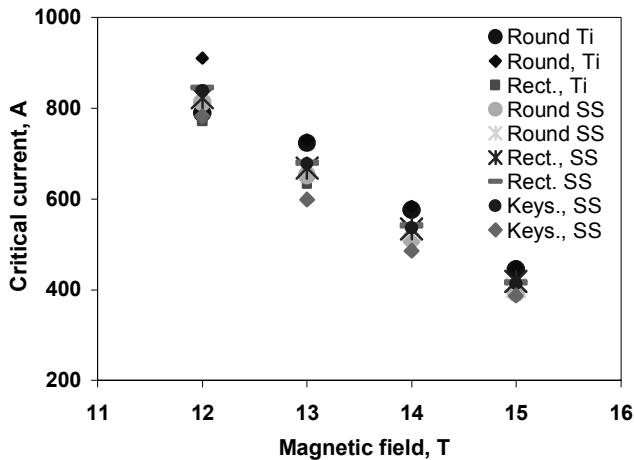

Fig. 4. I_c at high fields obtained through V-I measurements as a function of magnetic field for 1 mm 108/127 RRP round strands and strands extracted from cables. Ti and SS in legend represent test barrel material.

The measured I_S degradation was always less than 10%. The smallest I_S observed in V-H measurements on single strands was 975±25 A. To verify stability margins, two KS cable samples (one just insulated, and one insulated and epoxy impregnated) were tested at self-field up to 2 T with a SC transformer [13]. The impregnated cable was tested first, but despite pushing the transformer to its ~28 kA limit, this cable never quenched. On the other hand, the second tested sample showed a few quenches just above 28 kA. The quench current per strand of ~1000 A was very consistent with the minimum I_S value found in the strand tests.

V. RACETRACK COIL TEST

A 15 m long piece of KS cable was used to wind the small double-layer racetrack coil SR03. This coil allows testing a quite long piece of cable under magnet fabrication and operating conditions at self-field up to 11 T. The cable was insulated with ceramic tape. To wind flat coils from a keystoned cable, special spacers (folded ceramic tape with tapered size) were inserted between turns during winding. The coil was reacted in a three-step cycle recorded by type K thermocouples as detailed in Table IV. For these coils the duration of the high temperature step was reduced to 50 h. A picture of the reacted coil is shown in Fig. 5. After reaction the coil was impregnated with CTD101K epoxy at 60°C and then cured at 125°C for 21 hours. The details of SR design and fabrication are reported in [14].

TABLE IV
SR03 THERMAL CYCLE

Step	Time^a, h	Coil Ave. T, °C	Witness Ave. T, °C
RT to 205°C	12.3 / 12.25		
205- 215°C	80.0 / 80.3	215± 2	216± 2
215°C to 390°C	4.3 / 4.15		
390- 410°C	47 / 47	405± 2	405± 2
410°C to 640°C	3.15 / 3.25		
640-650°C	50 / 50	647± 3	648± 3

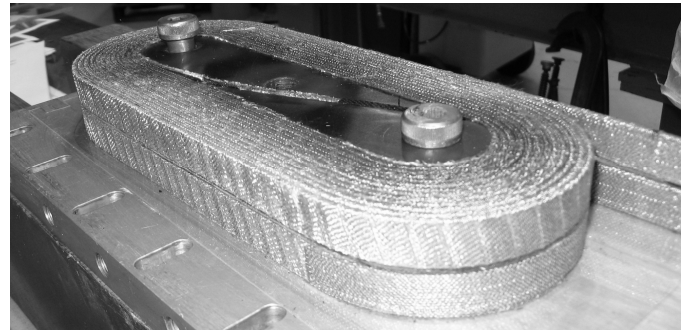^{a} Time for coil/ time for witness samples.

Fig. 5. Double-layer racetrack coil. Both layers are wound from a single piece of cable in the same direction.

SR03 was tested in boiling liquid He at 4.5 and 2.2 K. The quench history of SR03 is shown in Fig. 6. At 4.5 K the first training quench was at 18.68 kA at a nominal ramp rate of 20 A/s. After a relatively short training at 4.5 K (quenches 4-11 were caused by trips of the quench detection system), SR03 reached a plateau at 26.7-26.9 kA. Then the magnet was cooled down to 2.2 K and quenched several times at currents as high as 27.5-28 kA, which exposed the coil to larger Lorentz forces. However, at 2.2 K a stable quench plateau was not reached at a current ramp rate of 20 A/s due to quenches originating at the power leads. When warmed up to 4.5 K again, the magnet demonstrated the same maximum quench current of 26.98 kA.
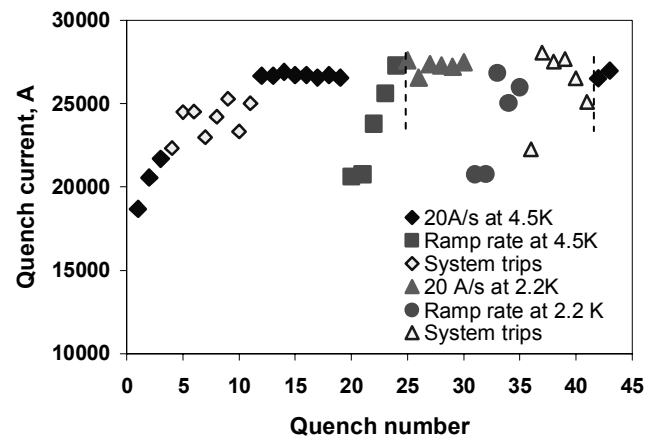

Fig. 6. SR03 quench history.

Results of a ramp rate dependence study at 4.5 and 2.2 K are summarized in Fig. 7. At 4.5 K the quench current as a function of the current ramp rate was a smooth curve with all quenches starting in the coil. At 2.2 K the quenches at current ramp rates above 50 A/s started in the magnet coil, and at lower ramp rates at the power leads outside the magnet.
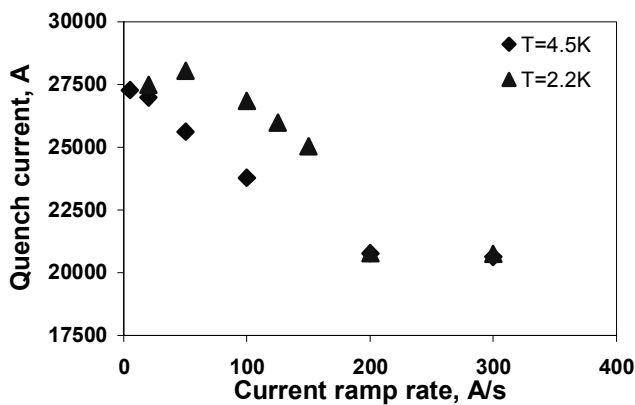
Fig. 7. SR03 ramp rate dependence at 4.5 and 2.2 K.

Training and ramp rate studies show that SR03 short sample limit at 4.5 K and 0 A/s is about 27.2 kA. At 2.2 K, its extrapolated short sample limit is about 29.2 kA.

Since quenches started at about the same time in both coil layers, it was not possible to pinpoint which coil was responsible for the quench. This indicates that the strand critical current on the narrow cable edge (remove "with larger strand deformation") is close to that at the thicker edge. The RRR measurement was performed during a gradual magnet warm up. The measured RRR value for SR03 was 173±10.

Round and extracted strands on both Ti and SS barrels were included as witnesses during the reaction of SR03 to evaluate the coil short sample limits (SSL). The average I_c, I_S and RRR results for several witness samples are shown in Table V.

TABLE V
WITNESS STRAND I_c (A) TEST RESULTS

Strand ID	15 T	14 T	13 T	12 T	Is, A	RRR
Round on Ti	472±3	606±6	747	(928±4)[a]	1675±25	175±3
Extr. on Ti	410±4	514±7	640±9	787±15	1525±25	156±2
Round on SS	435±2	559±8	716	891	1725±25	198±13
Extr. on SS	424±2	547±4	684±9	846±12	1575±25	162±0

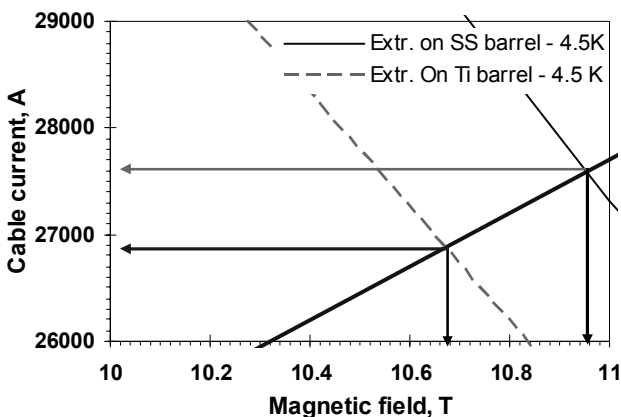[a] Extrapolated from the V-I curve.

Fig. 8. SR03 short sample limits at 4.5 K.

Given some difference in the currents measured on Ti and on SS barrels, two values of the coil short sample limit were derived from extracted strands tested on both kinds of barrels. The $I_c(B,T)$ curve was parameterized using [15], and the critical surfaces for the cable were then obtained at 4.5 K (see

Fig. 8). The SSL at 4.5 K was 26.9 kA from samples tested on Ti, and 27.6 kA from those tested on SS. This corresponds to a field on the coils of 10.7-11 T. The calculated SSL at 2.2 K is within 28.7 to 29.4 kA. The calculated ranges of SSL are in good agreement with the magnet test results at both temperatures. Witness sample RRR was 159±4, which also is in good agreement with the coils value.

VI. CONCLUSION

A 108/127 stack RRP strand was developed by OST and tested at Fermilab using 1.0 and 0.7 mm round and deformed strand samples. The reduction of filament size in the 1 mm strand combined with RRP technology optimization allowed reducing flux jumps and improving stability of this conductor preserving at the same time high values of critical current density and RRR. The 0.7 mm strand of this design requires further optimization to reduce the large RRR and I_S degradation due to deformations during rolling and cabling.

Rutherford cables made of 1 mm strand demonstrated good stability and low degradation of strand parameters. A small two-layer racetrack coil made of 27-strand cable reached its short sample limits at 4.5 K, producing a field of 11 T. The work on the optimization of this strand design will continue.

REFERENCES

[1] A.V. Zlobin, et al., "R&D of Nb₃Sn Accelerator Magnets at Fermilab", IEEE Trans. on Applied Superconductivity, Vol. 15, No. 2, 2005, p. 1113.
[2] A.V. Zlobin et al., ""Development and Test of Nb₃Sn Cos-theta Dipoles Based on PIT Strands", IEEE on Applied Superconductivity, Vol. 15, No. 2, 2005, p. 1160.
[3] S. Feher et al.. "Development and Test of Nb₃Sn Cos( ) Magnets Based on RRP and PIT Strands", IEEE Trans. on Applied Superconductivity, Vol. 16, No. 2, 2006, p. 315.
[4] F. Nobrega et al., "Nb₃Sn Accelerator Magnet Technology Scale Up Based on Cos-theta Coils", this conference.
[5] J.A. Parrell et al., "High field Nb₃Sn conductor development at Oxford Superconducting technology", IEEE Trans. on Applied Superconductivity, Vol. 13, No. 2, 2003, p. 3470.
[6] E. Barzi et al., "Instabilities in Transport Current Measurements of Nb₃Sn Strands", IEEE Trans. on Applied Superconductivity, Vol. 15, No. 2, 2005, p. 3364.
[7] A.K. Ghosh et al., "Investigation of Instability in High Jc Nb₃Sn Strands", IEEE Trans. on Applied Superconductivity, Vol. 15, No. 2, 2005 , p.3360.
[8] D. Turrioni et al., "Study of Effects of Deformation in Nb₃Sn Multifilamentary Strands", this conference.
[9] S. Hong et al., "Latest Improvements of Current Carrying Capability of Niobium Tin and Its Magnet Applications", IEEE Trans. on Applied Superconductivity, Vol. 16, No. 2, 2005, p. 1146.
[10] M.N. Wilson and C.R. Walters, "Magnetization and Stability Measurements", J. Phys. D, Appl. Phys., Vol. 13, 1970, p.1547.
[11] C. Boffo and E. Barzi, "Magnetization Measurements at the SSTF", FNAL Technical note, TD-99-036, 1999.
[12] N. Andreev et al., "Development of Rutherford-type Cables for High Field Accelerator Magnets at Fermilab", this conference.
[13] E. Barzi et al., "Study of Nb₃Sn Cable Stability at Self-field using a SC Transformer", IEEE Trans. on Applied Superconductivity, Vol. 15, No. 2, 2005, p. 1537.
[14] S. Feher et al., "Cable Testing for Fermilab`s High Field Magnets Using Small Racetrack Coils", IEEE Trans. on Applied Superconductivity, Vol. 15, No. 2, 2005, p.1550.
[15] L. T. Summers et al., "A model for the prediction of Nb₃Sn critical current as a function of field, temperature, strain and radiation damage", IEEE Trans. on Magnetics, Vol.27, No.2, 1991, p.2041.